Development of Phase Change Model of Heat Structure for the SPACE Code

Seung Wook Lee*, Jong Hyuk Lee, Jaeseok Heo, Sung Won Bae and Kyung-Doo Kim
Korea Atomic Energy Research Institute, 111 Daedeok-Daero 989 Beon-gil, Yuseong-gu, Daejeon, Korea
**Corresponding author: nuclist@kaeri.re.kr*

1. Introduction

When the reactor power excursion due to a reactivity-initiated accident occurs, the temperature of the fuel pellet increases very rapidly and may even excess the melting temperature of the pellet. Once the pellet temperature reaches the melting temperature, the phase change from solid to liquid occurs at the melting temperature. Such a melting process model may not be required for the analysis of the design basis accidents (DBAs) but is essential for the analysis of the design extension conditions (DECs). However, the current conduction model of the SPACE code cannot simulate the melting process. Therefore, an additional processing model for the SPACE [1] code is required to simulate the melting process in the reactor components during a transient for the analysis of the DEC scenarios.

2. Current Heat Structure Model of SPACE

There are two kinds of the heat conduction model in the SPACE code. First one is a one-dimensional heat conduction model and the other is a two-dimensional heat conduction model. The phase change model has been applied to the one-dimensional heat conduction model only because the two-dimensional heat conduction model is applied to the loss-of-coolant accident analysis where no pellet melting is expected. The heat conduction equation of the SPACE code is as follows:

$$\int_V \rho C_p \frac{\partial T}{\partial t} dV = \int_S k \nabla T \cdot d\hat{s} + \int_V q''' dV \tag{1}$$

where

ρC_p : volumetric heat capacity,
k : thermal conductivity,
V : volume,
S : surface area
q''' : volumetric heat source

Finite difference method (FDM) is used to get the heat conduction solutions. The spatial dependence of the internal heat source and the material may vary over each mesh interval. User can apply several kinds of the boundary conditions such as symmetry or insulated conditions, a correlation package, tables of surface temperature versus time, heat flux versus time, and heat transfer coefficient versus time. Fig. 1 shows a concept of the mesh points where the temperatures are defined and mesh intervals where the heat source and material properties are defined. The red-dashed line in Fig. 1 means the control volume of the m[th] mesh point.

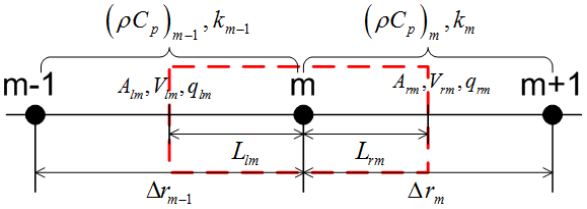

Fig. 1. Concept of mesh points and mesh intervals

Eq. 2 shows a finite difference form of Eq. 1 by using the definition of the spatial structure shown in Fig. 1.

$$\begin{aligned}\left(T_m^{n+1} - T_m^n\right)\frac{F_m}{\Delta t} = {} & \left(T_{m-1}^{n+1} - T_m^{n+1}\right)k_{m-1}\frac{A_{lm}}{\Delta r_{m-1}} \\ & + \left(T_{m+1}^{n+1} - T_m^{n+1}\right)k_{m+1}\frac{A_{rm}}{\Delta r_m} + q_{lm}V_{lm} + q_{rm}V_{rm}\end{aligned} \tag{2}$$

where

$$F_m = \left(\rho C_p\right)_{m-1} V_{lm} + \left(\rho C_p\right)_m V_{rm}$$

3. Phase Change Model

During a phase change, the temperature of a material is maintained at the melting temperature due to a large heat of fusion, whereas the enthalpy is changed. However, as shown in Eq. 2, current FDM of the SPACE cannot treat a melting process properly because Eq. 2 has no term related with the enthalpy change. For considering this effect, we introduced an explicit enthalpy equation as shown in Eq. 3 which is similar to the phase change model of the FRAPTRAN [2].

$$\begin{aligned}\rho H_M \left(V_{lm} + V_{rm}\right)\frac{\alpha_m^{n+1} - \alpha_m^n}{\Delta t} = {} & \left(T_{m-1}^{n+1} - T_{melt}\right)k_{m-1}\frac{A_{lm}}{\Delta r_{m-1}} \\ & + \left(T_{m+1}^{n+1} - T_{melt}\right)k_{m+1}\frac{A_{rm}}{\Delta r_m} \\ & + q_{lm}V_{lm} + q_{rm}V_{rm} + q_b A_b\end{aligned} \tag{3}$$

where

α_m : melting fraction,
H_M : heat of fusion or latent heat,
T_{melt} : melting temperature,
$q_b A_b$: boundary heat flow (if needed)

Comparing Eq. 3 with Eq. 2, the left hand side (LHS) of Eq. 3 is described using the enthalpy and melting

fraction and, the temperatures of the m^{th} mesh point in the right hand side (RHS) are replaced with the melting temperature. Eq. 3 is used to calculate melting fraction of the control volume when the structure temperature reaches the melting temperature.

To take account of the effect of the heat of fusion during a phase change, the volumetric heat capacity in Eq. 2 is replaced with a large value (~10^{30}) to make the mesh temperature remain equal to the melting temperature. The thermal conductivity is also modified considering the melting fraction.

When the temperature exceeds the melting temperature for the first time, initial melting fraction is determined by using the excess enthalpy as shown in Eq. 4.

$$\alpha_0 = \frac{H_{excess}}{H_M} = \frac{C_p\left(T_m^{n+1}\right)T_m^{n+1} - C_p\left(T_{melt}\right)T_{melt}}{H_M} \quad (4)$$

where

α_0 : initial melting fraction,

H_{excess} : excess enthalpy

Once melting or solidification process is completed, the temperature is determined by Eq. 5 considering the excess melting fraction.

$$T_m^{n+1} = T_{melt} + \frac{H_M\left(\alpha_m^{n+1} - \alpha_L\right)}{C_{p,L}} \quad (5)$$

where α_L is a limit of melting fraction and $C_{p,L}$ is a limit of specific heat. Each value of α_L and $C_{p,L}$ is dependent upon the phase change process as shown in Table I.

Table I: value of α_L and $C_{p,L}$

	melting ($\alpha_m^{n+1} > 1$)	freezing ($\alpha_m^{n+1} < 0$)
α_L	1	0
$C_{p,L}$	$C_{p,liquid}$	$C_{p,solid}$

After completion of the phase change, the temperature is calculated by using Eq. 2 again but the material properties corresponding to the state of material (solid or liquid) are used.

4. Validation

To validate the enthalpy-based phase change model, Stefan's problem [3] was selected as a validation problem. Fig. 2 shows the typical geometry for Stefan's problem. The phase change material (PCM) is semi-infinite, initially solid at its melting temperature (T_m), and at t = 0, the left wall temperature (T_b) is raised to $T_b > T_m$, prompting the PCM to start melting in a linear fashion starting at x = 0 by pure conduction. An insulated condition was applied for the right boundary condition. To apply the temperature boundary condition to the left side, a very small artificial mesh point of which the interval size (~10^{-6} m) is much smaller than those of regular intervals was added to the left boundary as shown in Fig. 2.

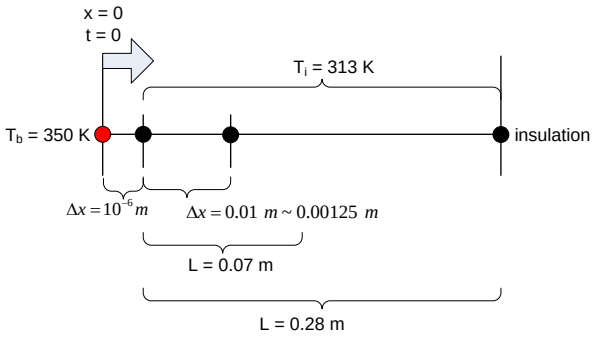

Fig. 2. 1-D conductor model for Stefan's problem

The size of total dimension is 0.28 m but the problem domain is restricted to 0.07 m to satisfy the semi-infinite condition of Stefan's problem. Table II shows the mesh information of each case and thermal properties of paraffin was obtained from the reference [3].

Table II: Condition of validation tests

Case	# of mesh*	Size of interval
1	30	0.01 m
2	58	0.005 m
3	114	0.0025 m
4	226	0.00125 m

* including the artificial mesh point

Test results from Fig. 4 to Fig. 7 show the temperature behavior of each test case. Symbols and lines in each figure represent the analytical solutions [3] and the calculation results, respectively. From the figures, it is found that the temperature behavior is very sensitive to the mesh size and the accuracy of the temperature behavior increased as the number of meshes increased because of the characteristic of the conduction equation. If the volume of mesh intervals is large, the enthalpy and time duration required for the complete melting increase, therefore, a step-wise temperature behavior is clearly shown in the coarse mesh. However, the result of the melting front location, which is an indicator of the melting fraction, is much more accurate compared with the temperature behavior as shown in Fig. 3. Even the result of the coarsest interval (N=28) is very close to the analytical solution, so that the phase change model based on the enthalpy change is applicable to the melting fraction calculation for the case of coarse mesh.

5. Conclusions

The phase change model based on the enthalpy change has been developed and validated through the comparison with the analytical solution of Stefan's problem. Although the calculation results were dependent on the number of mesh points, overall behavior of the results showed a good agreement with that of the analytical solutions for the temperature and melting front location during a transient. Therefore, the phase change model developed by this project can be applied to melting analysis of the major reactor components such as a reactor pressure vessel as well as fuel rod. In addition, to extent the applicable range of this model, it is required that the phase change model for the 2-D conduction model should be developed near future.

ACKNOWLEDGEMENT

This work was supported by the Nuclear Research & Development of the Korea Institute of Energy Technology and Planning(KETEP) grant funded by the Korea government Ministry of Trade, Industry and Energy.

(No. 20161510101840)

REFERENCES

[1] S. J. Ha *et al.*, A. R. Dulloo, J. G. Seidel, F. W, Hantz, and L. R. Grobmyer, Development of the SPACE Code for Nuclear Power Plants, Nuclear Engineering and Technology, Vol.43, No.1, 2011.
[2 K. J. Geelhood *et al*., FRAPTRAN-1.5: A Computer Code for the Transient Analysis of Oxide Fuel Rods, NUREG/CR-7023, Vol.1, Rev.1, USNRC, 2014.
[3] Wilson Ogoh and Dominic Groulx, Stefan's Problem: Validation of a One-Dimensional Solid-Liquid Phase Change Heat Transfer Process, COMSOL Conference 2010 Boston, Newton, MA, USA, 2010.

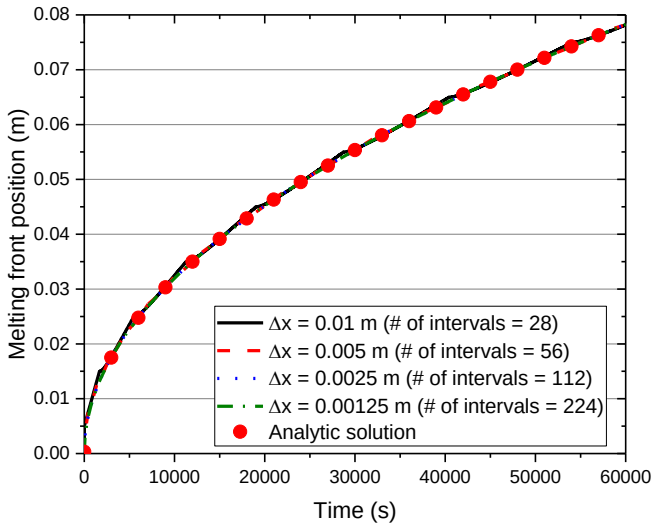

Fig. 3. Melting front location

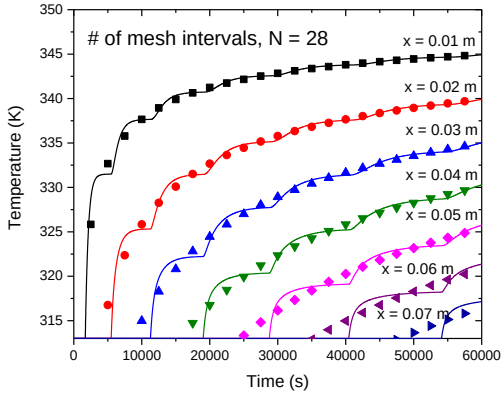

Fig. 4. Temperatures of Case 1

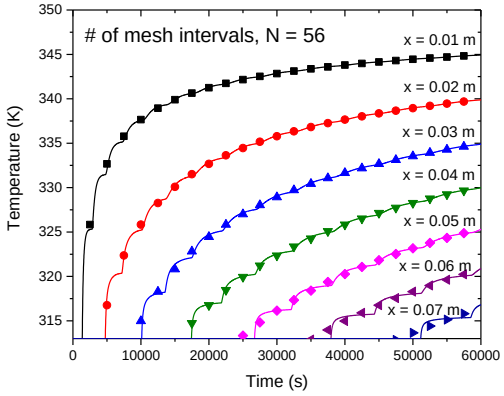

Fig. 5. Temperatures of Case 2

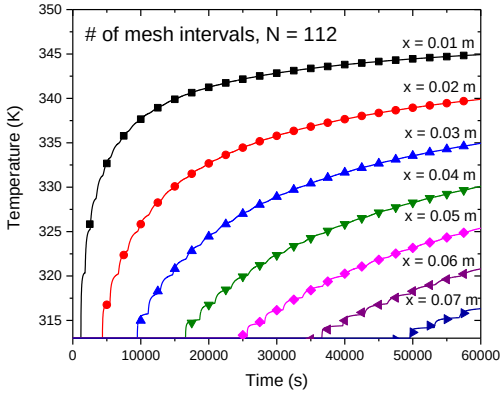

Fig. 6. Temperatures of Case 3

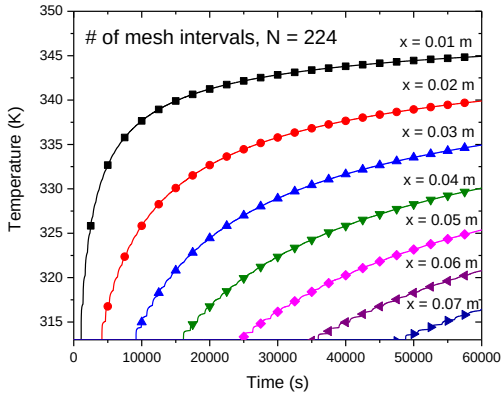

Fig. 7. Temperatures of Case 4